ORIGINAL ARTICLE

Phosphorylation of Lamin A/C at serine 22 modulates Na$_v$1.5 function

Michael A. Olaopa PhD[1,2] | **Tomohiko Ai MD, PhD**[2,3] | **Bo Chao PhD**[1] |
Xiangshu Xiao PhD[1] | **Matteo Vatta PhD**[2] | **Beth A. Habecker PhD**[1] ●

[1]Department of Chemical Physiology and Biochemistry, Oregon Health & Science University, Portland, Oregon, USA

[2]Krannert Institute of Cardiology, Department of Medicine, Indiana University School of Medicine, Indianapolis, Indiana, USA

[3]Department of Clinical Laboratory Medicine, Juntendo University, Tokyo, Japan

Correspondence
Beth A. Habecker PhD, Department of Chemical Physiology and Biochemistry, L334, Oregon Health and Science University, 3181 SW Sam Jackson Park Rd, Portland, OR 97239, USA.
Email: habecker@ohsu.edu

Abstract

Variants in the *LMNA* gene, which encodes for Lamin A/C, are associated with cardiac conduction disease (CCD). We previously reported that Lamin A/C variants p.R545H and p.A287Lfs*193, which were identified in CCD patients, decreased peak I_{Na} in HEK-293 cells expressing Na$_v$1.5. Decreased peak I_{Na} in the cardiac conduction system could account for patients' atrioventricular block. We found that serine 22 (Ser 22) phosphorylation of Lamin A/C was decreased in the p.R545H variant and hypothesized that lamin phosphorylation modulated Na$_v$1.5 activity. To test this hypothesis, we assessed Na$_v$1.5 function in HEK-293 cells co-transfected with *LMNA* variants or treated with the small molecule LBL1 (lamin-binding ligand 1). LBL1 decreased Ser 22 phosphorylation by 65% but did not affect Na$_v$1.5 function. To test the complete loss of phosphorylation, we generated a version of *LMNA* with serine 22 converted to alanine 22 (*S22A-LMNA*); and a version of mutant *R545H-LMNA* that mimics phosphorylation via serine 22 to aspartic acid 22 substitution (*S22D-R545H-LMNA*). We found that *S22A-LMNA* inhibited Lamin-mediated activation of peak I_{Na} by 63% and shifted voltage-dependency of steady-state inactivation of Na$_v$1.5. Conversely, *S22D-R545H-LMNA* abolished the effects of mutant *R545H-LMNA* on voltage-dependency but not peak I_{Na}. We conclude that Lamin A/C Ser 22 phosphorylation can modulate Na$_v$1.5 function and contributes to the mechanism by which *R545H-LMNA* alters Na$_v$1.5 function. The differential impact of complete versus partial loss of Ser 22 phosphorylation suggests a threshold of phosphorylation that is required for full Na$_v$1.5 modulation. This is the first study to link Lamin A/C phosphorylation to Na$_v$1.5 function.

KEYWORDS
cardiac conduction disease, Lamin phosphorylation, Na$_v$1.5

1 | INTRODUCTION

Laminopathies are a broad spectrum of diseases involving cardiac and skeletal anomalies attributed to mutations in the *LMNA* gene, which encodes for Lamin A/C. These disorders comprise over 12 clinically heterogeneous syndromes (Bertrand et al., 2011). Lamin A/C is a type-V intermediate filament that forms the nuclear lamina underlying the inner membrane of the nucleus (Houben et al., 2013). *LMNA* mutations are highly prevalent in patients with cardiac conduction disease (CCD), often associated with eventual dilated cardiomyopathy (DCM; Anselme et al., 2013; Barra et al., 2012; Hermida-Prieto et al., 2004; Keller et al., 2012; Malek et al., 2011; Mounkes et al., 2005; Olaopa et al., 2018; Saj et al., 2010; Shaw et al., 2002; Zaragoza et al., 2016). A clinical study of familial autosomal DCM found that approximately 33% of patients were positive for *LMNA* mutations (Arbustini et al., 2002). *LMNA* patients require implantable cardioverter-defibrillator or pacemaker therapy to prevent cardiac arrest and sudden death (Anselme et al., 2013; Kumar et al., 2016; Olaopa et al., 2018). The clinical presentations of these patients, including atrioventricular (AV) block and progressive CCD, are similar to those observed in disorders caused by mutations in the *SCN5A* gene (Olaopa et al., 2018; Wang et al., 2002), which encodes for the cardiac sodium channel (Na$_v$1.5).

Na$_v$1.5 is primarily localized within the sarcolemma, in contrast to the nuclear localization of Lamin A/C. Mutations in *SCN5A* are a major cause of AV block, sick sinus syndrome, progressive CCD, and eventual DCM leading to sudden death (Amin et al., 2010; Chockalingam et al., 2012; Holst et al., 2010; Lee et al., 2016; Makita, 2009; Samani, Ai, et al., 2009; Samani, Wu, et al., 2009; Shuraih et al., 2007). Due to the similarities between clinical presentations of disorders associated with both *LMNA* and *SCN5A* mutations, studies by our group and others have sought to functionally link variants in Lamin A/C to Na$_v$1.5 activity (Liu et al., 2016; Markandeya et al., 2016; Olaopa et al., 2018). Our group reported that two Lamin A/C variants (p.R545H and p.A287Lfs*193), found in patients with CCD, significantly decrease peak sodium current (I_{Na}) and shift the voltage-dependency of steady-state inactivation of Na$_v$1.5 (Olaopa et al., 2018). The p.R545H variant is due to a missense point mutation (c.1634G>A); while the p.A287Lfs*193 variant is caused by a single nucleotide deletion (c.859delG) and subsequent frame shift, leading to a premature termination codon (Olaopa et al., 2018).

Although the transcriptional and post-translational regulation of Lamin A/C within the heart is not fully understood, its phosphorylation has functional importance (Buxboim et al., 2014; Haas & Jost, 1993; Kochin et al., 2014; Mitsuhashi et al., 2010; Swift & Discher, 2014; Torvaldson et al., 2015; Wu et al., 2011). Phosphorylation at serine 22 (Ser 22) plays an important role in cell cycle regulation, nuclear stability, and signaling between the nucleoskeleton and cytoskeletal structures––the LINC (Linker of Nucleoskeleton and Cytoskeleton) complex (Buxboim et al., 2014; Kochin et al., 2014; Osmanagic-Myers et al., 2015; Swift & Discher, 2014; Torvaldson et al., 2015). Additionally, a p.S22L Lamin A/C variant was identified in a genetic screen of cardiac transplant patients with DCM (Pethig et al., 2005), indicating a clinically relevant role for Ser 22 in cardiac disease. Thus, we sought to determine if Ser 22 is involved in the mechanism by which the p.R545H variant affects Na$_v$1.5 function, with the aim of identifying a potential therapeutic target for CCD patients with similar *LMNA* mutations. We used a novel small molecule (lamin-binding ligand, LBL1) that binds Lamin A/C in the N-terminal region encompassing Ser 22 (Chao et al., 2017; Li et al., 2018), as well as genetic (Ser 22 modification) approaches to modulate Ser 22 phosphorylation and determine its role in Na$_v$1.5 function.

2 | MATERIALS AND METHODS

2.1 | Cloning and generation of plasmids

The cDNA of wild-type *LMNA* (ORF NM_005572) was purchased (OriGene) in a pCMV6-AC-GFP (C-terminus fused) vector backbone. Mutant *R545H-LMNA* and phosphorylation *LMNA* constructs (*S22A-LMNA* and *S22D-R545H-LMNA*) were generated using site-directed mutagenesis kit (Qiagen). We substituted alanine (GCG) for serine (TCG) at position 22 (p.S22A) in wild-type *LMNA* to prevent phosphorylation; to mimic phosphorylation in the *R545H-LMNA* mutant we substituted aspartic acid (GAC) for serine (TCG) at position 22 (p.S22D) in the *R545H-LMNA* plasmid. DNA sequencing and western blot analyses confirmed successful mutagenesis (Figure 1).

2.2 | Cell culture and transfection

HEK-293 cells were grown and maintained in DMEM media (Thermo Fisher), supplemented with 10% fetal bovine serum (ATCC). Cells were serum-starved overnight and transiently transfected with identical amounts of plasmid DNA using Effectene (Qiagen). Cells were treated 24 hrs post-transfection with vehicle dimethyl sulfoxide (1% DMSO), 5 or 10 μM LBL1. Cells were harvested 24 hrs post-treatment or 48 hrs post-transfection.

FIGURE 1 Confirmation of *LMNA* phosphorylation plasmids. (a) Electropherographs of sequencing results confirming mutagenesis of targeted codon (blue highlight) for each respective *LMNA* phosphorylation plasmid. (b) Western blot on protein lysates extracted from HEK-293 cells transfected with each respective *LMNA* plasmid
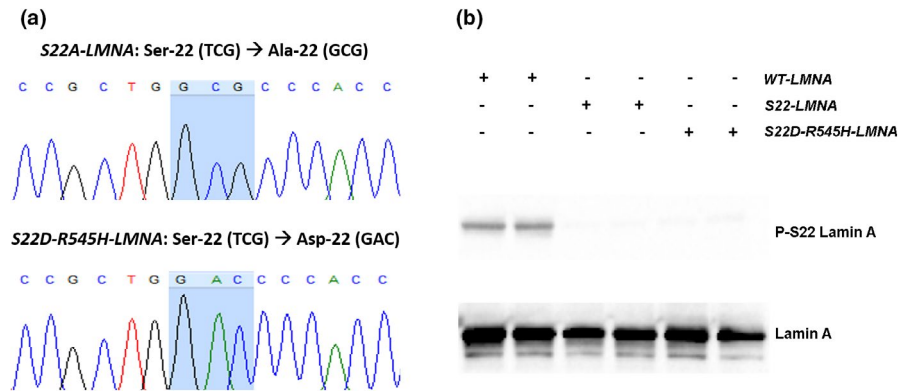
2.3 | Protein isolation and western blot

Protein was isolated in lysis buffer (in mM): Tris 20, etheylenediaminetetraacetic acid (EDTA) 10, NaCl 100, 1% SDS, 1× complete protease inhibitor (Roche), and 1× phosphatase cocktail inhibitor (Sigma Aldrich). SDS-PAGE used 4%–15% gradient Tris–HCl polyacrylamide precast gels in 1× Tris/Glycine/SDS running buffer (Bio-Rad). For high molecular weight proteins, overnight wet transfer was performed (20 V, 16 h); for medium and low molecular weight proteins, fast semi-dry transfer was performed (25 V, 40 min) using a Novex Semi-Dry Blotter apparatus (Invitrogen). Transfers were onto nitrocellulose membranes (GE Life Sciences). Primary antibodies : mouse monoclonal anti-pan-sodium channel (1:500) and anti-beta-tubulin (1:10,000; Sigma-Aldrich); rabbit anti-total-lamin (1:2000), anti-phospho-lamin (Ser 22, 1:2000), and anti-alpha-actinin 2 (1:2000) (Cell Signaling). Secondary antibodies (Thermo Fisher): goat anti-mouse-HRP (1:5000) and goat anti-rabbit-HRP (1:5000). Primary antibodies were incubated overnight at 4°C. Secondary antibodies were incubated at room temperature for 1 h, developed using SuperSignal West Pico or Femto (Thermo Fisher), and imaged using ChemiDoc XRS+ (Bio-Rad). Membranes were stripped with Restore Stripping buffer (Thermo Fisher) at 55°C for 15 min followed by shaking at room temperature for 30 min. Antibody and blocking solutions were prepared in 0.1% Tween-20 in Tris-buffered saline solution (in mM): NaCl 150, Tris 10 (pH 7.4). Bands were quantified with ImageJ (NIH).

2.4 | Patch clamp experiments

Cells were harvested using trypsin-EDTA (Thermo Fisher) for 2 min and transferred to the patch chamber for whole-cell recording of GFP-labeled cells, which was performed as previously described (Olaopa et al., 2018; Yu et al., 2014). Whole-cell configuration was made in bath solution (in mM): NaCl 140, KCl 5, CaCl$_2$ 1.8, MgCl$_2$ 1, 4-(2-hydro xyethyl)-1-piperazineethanesulfonic acid (HEPES) 5, and Glucose 10 (pH 7.4 adjusted with NaOH). Pipette resistances were 1.5–3 MΩ; solution (in mM): NaF 10, CsF 110, CsCl 20, ethylene glycol tetraacetic acid (EGTA) 10, and HEPES 10 (pH 7.35 adjusted with CsOH). After achieving a giga-seal, the test pulse current was nulled by adjusting the pipette capacitance compensator with both fast and slow components. After break-in, the whole-cell charging transient was nulled by adjusting whole-cell capacitance and series resistance. Voltage control protocols were generated with Axopatch 200B amplifier/Digidata 1440A or MultiClamp 700A acquisition system using pCLAMP-10 software (Molecular Devices). Whole-cell recording was analyzed using Clampfit 10.2 (Molecular Devices). All experiments were carried out at room temperature. Conductance G (V) was calculated by the equation:

$$G(V) = \frac{I}{(V_m - E_{rev})},$$

where I is the peak current, E_{rev} is the measured reversal potential, and V_m is the membrane potential. The normalized peak conductance was plotted as a function of membrane potentials. Steady-state inactivation was estimated by pre-pulse protocols (500 ms) from a holding potential of −140 mV. Steady-state activation and inactivation were fitted with the Boltzmann equation: $y = [1 + \exp((V_m - V_h)/k)] − 1$, where y represents variables; V_h, midpoint; k, slope factor; and V_m, membrane potential.

2.5 | Statistical analyses and data availability

The Mann–Whitney–Wilcoxon rank test was performed for patch clamp analyses. One-way ANOVA test was performed for western blot densitometry. For statistical significance $p < 0.05$ was used. Data are presented as mean ± SE. The data associated with this manuscript will be made available.

3 | RESULTS

3.1 | Mutagenesis of Ser 22 residue

We generated *LMNA* phosphorylation plasmids that either mimic loss of phosphorylation in wild type (*S22A-LMNA*) or constitutive phosphorylation in the *R545H-LMNA* mutant (*S22D-R545H-LMNA*). We selected the *R545H-LMNA* mutant for our study due to the previously described decrease in Ser 22 phosphorylation. To mimic loss of phosphorylation, we genetically substituted alanine (GCG codon) for serine (TCG codon) residue at position 22 (p.S22A); conversely, to mimic phosphorylation, we genetically substituted aspartic acid (GAC codon) for serine (TCG codon) residue at position 22 (p.S22D). We confirmed successful mutagenesis by sequencing and western blot (Figure 1). Cells that expressed either the *S22A-LMNA* or *S22D-R545H-LMNA* plasmids appeared negative for Ser 22 phosphorylation, indicating the serine residue had been successfully mutated.

3.2 | Ser 22 Lamin phosphorylation is reduced in *R545H-LMNA* mutant

We found that Ser 22 Lamin A/C phosphorylation was reduced by 60% in cells expressing *R545H-LMNA* compared to wild type (Figure 2a,c). The *A287Lfs-LMNA* mutation decreased total Lamin A/C levels but did not impact Ser 22 phosphorylation (Figure 2a,d) and was therefore not a subject of this study. *R545H-LMNA* did not alter $Na_v1.5$ whole-cell protein content (Figure 2b), indicating that the decrease in peak I_{Na} was not due to a change in total channel expression. We did not assess localization of $Na_v1.5$ to the membrane, and cannot rule out a role for decreased cell surface expression of sodium channels contributing to the decrease in peak I_{Na}. Alpha-actinin 2, which has been

shown to modulate $Na_v1.5$ function via direct interaction (Ziane et al., 2010), was likewise unchanged by *R545H-LMNA* (Figure 2b).

3.3 | Ablation of Ser 22 phosphorylation recapitulates *R545H-LMNA* effect on I_{Na}

R545H-LMNA, which decreased Ser 22 phosphorylation, also decreased peak I_{Na} and shifted voltage-dependency of steady-state inactivation rightward, with no effect on steady-state activation (Olaopa et al., 2018). To determine if Ser 22 Lamin A/C phosphorylation contributed to the regulation of $Na_v1.5$, we assessed peak I_{Na} in cells transfected with wild-type *LMNA* or *S22A-LMNA*, which cannot be phosphorylated on Ser 22. *S22A-LMNA* significantly decreased peak I_{Na} by 60% compared to wild-type *LMNA* (S22A: -125 ± 12 pA/pF, $N = 10$ vs. wild type: -339 ± 45 pA/pF, $N = 10$, $p < 0.0005$; Figure 3a,b). Similar to the *R545H-LMNA* mutant (Olaopa et al., 2018), *S22A-LMNA* also led to a rightward shift of steady-state of inactivation (*S22A*: $V_h = -88.10 \pm 0.51$ mV, $N = 7$ vs. wild type: $V_h = -93.20 \pm 0.89$ mV, $N = 10$, $p < 0.05$) while leaving steady-state activation unaltered (Figure 4a; Table 1).

3.4 | Mimicking Ser 22 phosphorylation in *R545H-LMNA* partially restores $Na_v1.5$ function

To test if Ser 22 played a role in the mechanism by which *R545H-LMNA* decreased peak I_{Na} (Olaopa et al., 2018), we generated a version of *R545H-LMNA* that substituted aspartic acid for serine at position 22 (*S22D-R545H-LMNA*) to mimic phosphorylation at that site. We then measured peak I_{Na} in cells transfected with *S22D-R545H-LMNA*. We
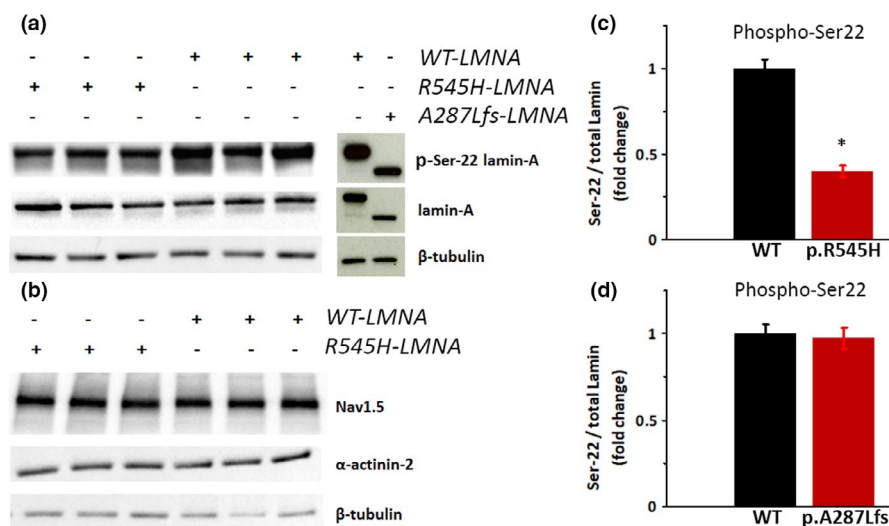

FIGURE 2 Serine 22 phosphorylation in *LMNA*-transfected cells. (a, b) Representative western blots of HEK-293 cells transfected with the combination of plasmids noted. (c, d) Densitometry showing fold change of Ser 22 phosphorylation in: (c) *WT-LMNA* ($N = 6$) and *R545H-LMNA* ($N = 6$); *$p < 0.05$. (d) *WT-LMNA* ($N = 6$) and *A287Lfs-LMNA* ($N = 4$); $p = $ N.S. Data are mean $\pm$ SE
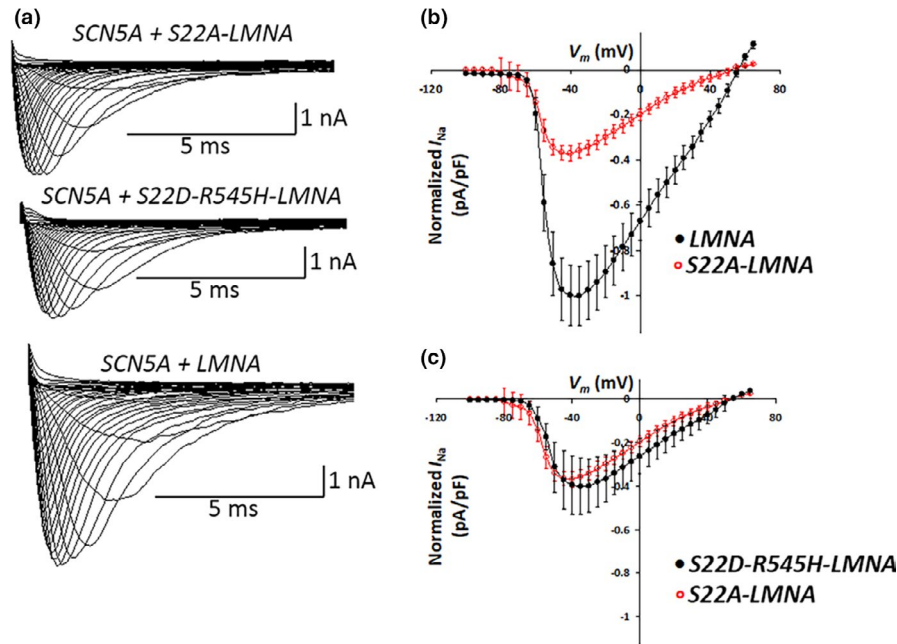
FIGURE 3 *S22A-LMNA* phosphorylation mutant alters peak I_{Na}. (a) Representative superimposed current traces drawn to scale obtained from cells co-transfected with *SCN5A* and LMNA variants; step-pulse protocol (inset). (b) I–V relationship comparing cells co-transfected with *SCN5A + WT-LMNA* (black), $N = 10$ versus *SCN5A + S22A-LMNA* (red), $N = 10$; $p < 0.0005$. Peak current for *SCN5A + WT-LMNA = 1*. (c) I–V relationship comparing cells co-transfected with *SCN5A + S22A-LMNA* (red), $N = 10$ versus *SCN5A + S22D-R545H-LMNA* (black), $N = 7$; $p = $ N.S. Peak current for *SCN5A + WT-LMNA* is set at 1
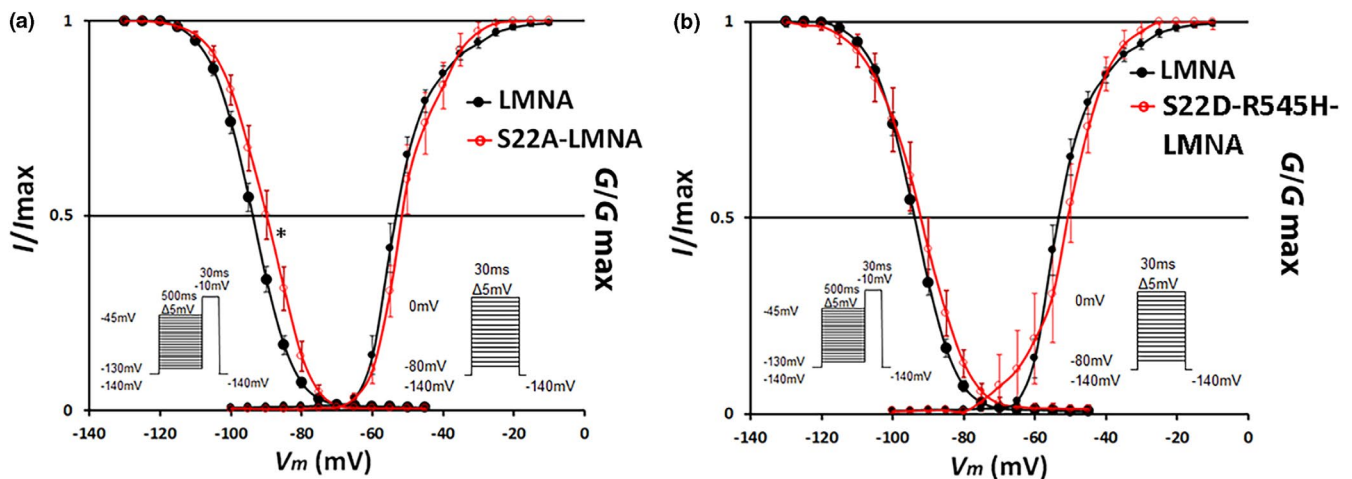

FIGURE 4 4 *S22A-LMNA* phosphorylation mutant alters steady-state inactivation. Voltage-dependency of the steady-state inactivation and activation of cells co-transfected with *SCN5A + WT-LMNA* (black) versus *SCN5A + S22A-LMNA* (red, a) or *S22D-R545H-LMNA* (red, b). Inactivation: *SCN5A + WT-LMNA* versus *SCN5A + S22A-LMNA* $p < 0.05$. No significant differences in other inactivation or activation curves. Insets show pre-pulse inactivation (left) and step-pulse activation (right) protocols. Data are mean ± SE

anticipated that *S22D-R545H-LMNA* would restore peak I_{Na} to the levels seen with wild-type *LMNA*. However, a similar loss of peak I_{Na} occurred in cells expressing *S22D-R545H-LMNA*, indicating that it was unable to rescue the *R545H-LMNA* effect on peak I_{Na} (*S22D-R545H*: -137 ± 44 pA/pF, $N = 7$ vs. *S22A*: -125 ± 12 pA/pF, $N = 10$, $p = $ N.S.; Figure 3a,c). In contrast, *S22D-R545H-LMNA* prevented the shift in the steady-state inactivation

of the voltage-dependency. Cells transfected with *S22D-R545H-LMNA* were indistinguishable from wild-type *LMNA* (Figure 4b; *S22D-R545H*: $V_h = -92.60 \pm 1.41$ mV, $N = 6$ vs. wild type: $V_h = -93.20 \pm 0.89$ mV, $N = 10$, $p = $ N.S.). Thus, mimicking Ser 22 phosphorylation partially rescued Na$_v$1.5 function disrupted by the *R545H-LMNA* mutation, as normal voltage-dependency was restored but peak I_{Na} levels were not (Table 1).

TABLE 1 Summary of I_{Na} parameters

	WT	LBL1 (10 μM)	p.S22A	p.S22D-R545H
I–V relationship	$N = 10$	$N = 7$	$N = 10$	$N = 7$
Peak I_{Na} (pA/pF)	-339 ± 45	-319 ± 26	$-125 \pm 12^{***}$	$-137 \pm 44^{***}$
Steady-state inactivation	$N = 10$	$N = 8$	$N = 7$	$N = 6$
V_h (mV)	-93.20 ± 0.89	-95.91 ± 1.72	$-88.10 \pm 0.51^{*}$	-92.60 ± 1.41
K	5.62 ± 0.07	7.42 ± 0.17	6.84 ± 0.16	7.23 ± 0.30
Steady-state activation	$N = 10$	$N = 7$	$N = 10$	$N = 7$
V_h (mV)	-52.38 ± 0.41	-55.92 ± 1.23	-50.21 ± 1.48	-51.70 ± 1.39
K	5.21 ± 0.36	5.37 ± 0.17	5.28 ± 0.22	6.62 ± 0.34

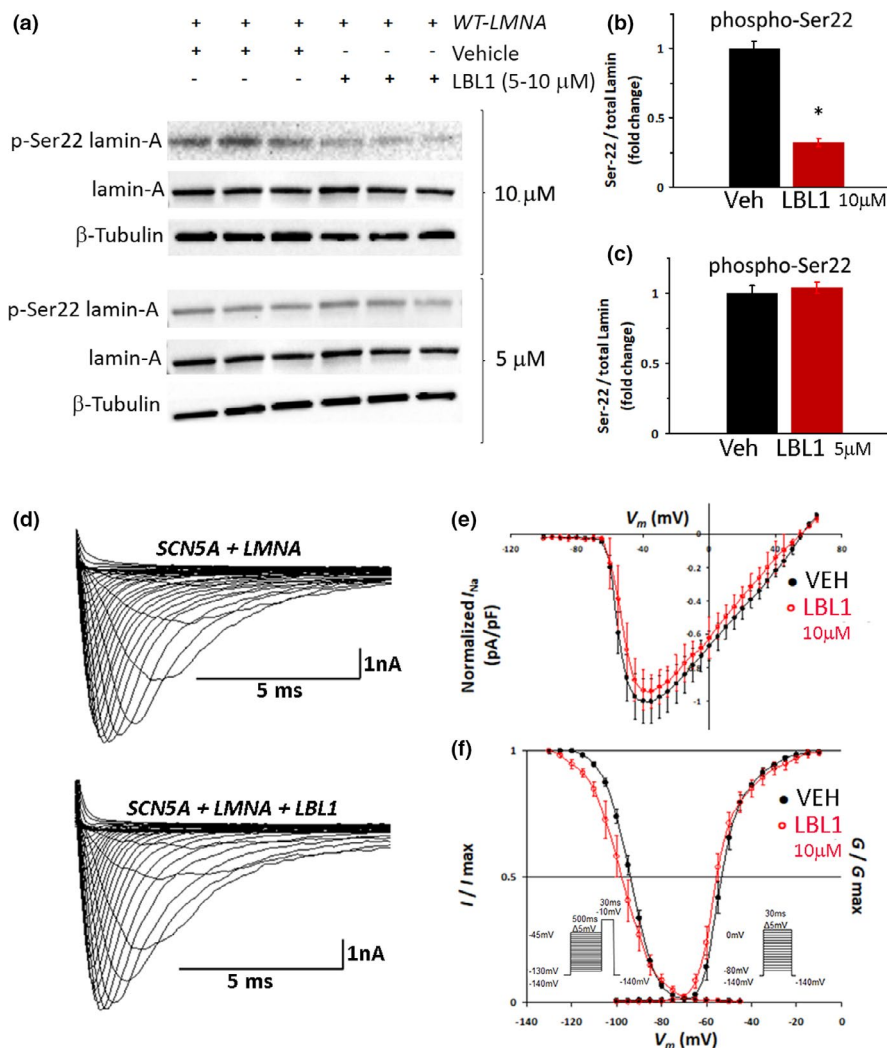$*p < 0.05$,; $***p < 0.0005$ (vs. WT).

FIGURE 5 LBL1 decreases Ser 22 Phosphorylation but does not alter I_{Na}. (a) Representative western blot of HEK-293 cells transfected with *WT-LMNA* and treated with 10 μM LBL1 (top) or 5 μM LBL1 (bottom). (b, c) Quantification of Ser 22 phosphorylation in cells treated with vehicle, 10 μM (b) or 5 μM (c) LBL1 (red bars). $N = 6$; $*p < 0.05$. Ser 22 phosphorylation in vehicle-treated cells was set at 1. (d) Representative superimposed current traces obtained from respective cells. (e) I–V relationship of cells co-transfected with *SCN5A + WT-LMNA*; vehicle (black), $N = 10$ versus 10 μM LBL1 (red), $N = 7$. Peak current for vehicle is set at 1. (f) Voltage-dependency of the steady-state inactivation and activation of cells co-transfected with *SCN5A + WT-LMNA*. Inactivation: vehicle (black), $N = 10$ versus 10 μM LBL1 (red), $N = 8$; $p = $ N.S. Activation: vehicle (black), $N = 10$ versus 10 μM LBL1 (red), $N = 7$; $p = $ N.S. Insets show pre-pulse inactivation (left) and step-pulse activation (right) protocols. Data are mean $\pm$ SE

3.5 | LBL1 inhibits Ser 22 phosphorylation but does not affect Na$_v$1.5 function

LBL1, which binds Lamin A/C in the N-terminal region encompassing Ser 22, was identified based on its ability to inhibit the growth of cancer cells (Chao et al., 2017; Li et al., 2018). LBL1 inhibits the proliferation of cancer cells at micromolar concentrations, so we treated *LMNA*-transfected HEK-293 cells with 5 and 10 μM LBL1 to determine if that was sufficient to prevent the phosphorylation of Ser 22. Treating *LMNA*-transfected cells with 10 μM LBL1

reduced Ser 22 phosphorylation by 65% while 5 µM LBL1 had no effect (Figure 5a–c). To determine the effect of LBL1-suppressed Lamin A/C phosphorylation on $Na_v1.5$ function, we assessed peak I_{Na} and voltage-dependency in cells treated with 10 µM LBL1 compared to vehicle. We anticipated that inhibition of Lamin Ser 22 phosphorylation would lead to changes in $Na_v1.5$ function similar to those seen with the *R545H-LMNA* or *S22A-LMNA* mutations. However, decreasing Ser 22 phosphorylation by LBL1 in wild-type Lamin did not change peak I_{Na} or steady-state inactivation or activation (Figure 5d–f; Table 1).

4 | DISCUSSION

The goal of this study was to understand the effect of Lamin A/C Ser 22 phosphorylation on $Na_v1.5$ function, with the aim of identifying a novel therapeutic target for CCD patients with *LMNA* mutations. Our findings indicate that Ser 22 phosphorylation plays a role in Lamin-mediated $Na_v1.5$ modulation and can alter peak I_{Na} and voltage-dependency of the steady-state inactivation. However, there appears to be a threshold level of phosphorylation necessary in wild-type Lamin A/C. Partial loss of Ser 22 phosphorylation via the lamin-binding small molecule LBL1 did not affect $Na_v1.5$ function, but complete loss of Ser 22 phosphorylation via genetic substitution had significant effects on channel function that were consistent with the *R545H-LMNA* variant (Table 1).

Another possible explanation for the discrepancy between the effect of partial and complete loss of Ser 22 phosphorylation is that other Lamin A/C phosphorylation sites, in addition to Ser 22, may play a cumulative role in modulating $Na_v1.5$. This alternative interpretation is supported by our findings, which show that mimicking constitutive Ser 22 phosphorylation in the *R545H-LMNA* mutant only partially restored Nav1.5 function. This suggests that there are other factors and/or phosphorylation sites that also play a role in governing the effect of *R545H-LMNA* or other *LMNA* mutations on sodium channel function or cell surface expression. To explore this possibility, future studies will be focused on assessing the role of additional Lamin A/C phosphorylation sites and developing chemical and genetic tools that can specifically identify and modulate these sites.

Lamin A/C is an intermediate filament organized into a tripartite structure: a non-helical N-terminal head domain encompassing the Ser 22 phosphorylation site; an α-helical coiled-coil rod domain encompassing the 287 residue; and an immunoglobulin fold (Ig-fold) domain at the C-terminal end encompassing the 545 residue (Ho & Lammerding, 2012; Osmanagic-Myers et al., 2015). The Ig-fold domain, which spans residues 430–545, is believed to be involved in Lamin A/C's protein–protein functional interactions (Dhe-Paganon et al., 2002; Krimm et al., 2002; Shumaker et al., 2008), including with cytoskeletal linkers that provide the machinery by which sarcolemma proteins like $Na_v1.5$ might be modulated (Markandeya et al., 2016; Olaopa et al., 2018; Stroud et al., 2014). Consistent with this, both the *R545H* and *A287Lfs* mutations alter the Ig-fold domain. *R545H* is a point mutation at the end of the Ig-fold, a location that has been implicated in other laminopathies including DCM and CCD with loss of peak I_{Na} (Chan et al., 2016; Liu et al., 2016; Malek et al., 2011; Saj et al., 2010). The *A287Lfs* frame shift mutation alters the sequence from A287 in the rod domain to the premature stop codon in the Ig-fold. In contrast, LBI1 binds Lamin A/C in the N-terminal region encompassing Ser 22 (Chao et al., 2017; Li et al., 2018).

Dimerization of Lamin A/C is driven by coiled-coil formation of its central rod domains (Ho & Lammerding, 2012) (Dhe-Paganon et al., 2002; Krimm et al., 2002; Stuurman et al., 1998). Lamin A/C dimers assemble head-to-tail into polar polymers, which require an overlapping interaction between the head and tail domains (Heitlinger et al., 1992; Sasse et al., 1998). These polymers then laterally assemble in an anti-parallel fashion into nonpolar filaments (Ben-Harush et al., 2009). These reports, in addition to our findings, lead us to propose a structural paradigm by which the *R545H* mutation could affect Ser 22 phosphorylation via antiparallel head-to-tail interaction with neighboring dimers (graphical abstract). In the case of the *A287Lfs* mutant, which does not result in loss of Ser 22 phosphorylation levels, this head-to-tail interaction is likely abolished due to the frame shift and subsequent truncation of this region of the protein. This truncation could explain why modulation of Ser 22 phosphorylation level does not occur in the *A287Lfs* mutant. The complex structure of lamin polymers may also explain why a twofold increase in LBL1 concentration induced a significant loss of Ser 22 phosphorylation. Experimental approaches aimed at exploring these possibilities, while important, are outside the scope and focus of this study.

From a clinical perspective, our results suggest that Lamin A/C phosphorylation may be a potential therapeutic target for patients with specific *LMNA* mutations and CCD. Small molecules that enhance, rather than block, Ser 22 phosphorylation might partially restore $Na_v1.5$ function in disease caused by *R545H* and similar *LMNA* mutations. This would mimic the partial rescue of $Na_v1.5$ function we observed in cells expressing the *S22D-R545H-LMNA* variant. It could also help to improve diagnosis and prognosis in patients with similar *LMNA* mutations by developing tools that could assess their Lamin A/C phosphorylation state.

In summary, our data indicate that Lamin A/C Ser 22 phosphorylation modulates Na$_v$1.5 function. This phosphorylation appears to be part of the mechanism by which the *R545H-LMNA* mutation affects Na$_v$1.5 function. To our knowledge, this is the first study to link Lamin A/C phosphorylation and Na$_v$1.5 function.

CONFLICT OF INTEREST
All authors declare no conflict of interest.

AUTHOR CONTRIBUTIONS
Michael A. Olaopa performed the research. Michael A. Olaopa and Tomohiko Ai performed the analyses. Michael A. Olaopa, Tomohiko Ai, Matteo Vatta, and Beth A. Habecker contributed to conceptualization and design of the study. Bo Chao, Xiangshu Xiao, and Beth A. Habecker contributed analytic tools and resources. Michael A. Olaopa wrote the manuscript with significant contributions from all co-authors. All authors reviewed and approved the final manuscript.

ORCID
Beth A. Habecker https://orcid.org/0000-0002-4658-8730

REFERENCES
Amin, A. S., Asghari-Roodsari, A., & Tan, H. L. (2010). Cardiac sodium channelopathies. *Pflugers Archiv. European Journal of Physiology*, *460*, 223–237. https://doi.org/10.1007/s00424-009-0761-0

Anselme, F., Moubarak, G., Savoure, A., Godin, B., Borz, B., Drouin-Garraud, V., & Gay, A. (2013). Implantable cardioverter-defibrillators in lamin A/C mutation carriers with cardiac conduction disorders. *Heart Rhythm: the Official Journal of the Heart Rhythm Society*, *10*, 1492–1498. https://doi.org/10.1016/j.hrthm.2013.06.020

Arbustini, E., Pilotto, A., Repetto, A., Grasso, M., Negri, A., Diegoli, M., Campana, C., Scelsi, L., Baldini, E., Gavazzi, A., & Tavazzi, L. (2002). Autosomal dominant dilated cardiomyopathy with atrioventricular block: A lamin A/C defect-related disease. *Journal of the American College of Cardiology*, *39*, 981–990. https://doi.org/10.1016/S0735-1097(02)01724-2

Barra, S. N., Providencia, R., Paiva, L., Nascimento, J., & Marques, A. L. (2012). A review on advanced atrioventricular block in young or middle-aged adults. *Pacing and Clinical Electrophysiology*, *35*, 1395–1405. https://doi.org/10.1111/j.1540-8159.2012.03489.x

Ben-Harush, K., Wiesel, N., Frenkiel-Krispin, D., Moeller, D., Soreq, E., Aebi, U., Herrmann, H., Gruenbaum, Y., & Medalia, O. (2009). The supramolecular organization of the *C. elegans* nuclear lamin filament. *Journal of Molecular Biology*, *386*(5), 1392–1402. https://doi.org/10.1016/j.jmb.2008.12.024

Bertrand, A. T., Chikhaoui, K., Yaou, R. B., & Bonne, G. (2011). Clinical and genetic heterogeneity in laminopathies. *Biochemical Society Transactions*, *39*, 1687–1692. https://doi.org/10.1042/BST20110670

Buxboim, A., Swift, J., Irianto, J., Spinler, K. R., Dingal, P. C., Athirasala, A., Kao, Y. R., Cho, S., Harada, T., Shin, J. W., & Discher, D. E. (2014). Matrix elasticity regulates lamin-A, C phosphorylation and turnover with feedback to actomyosin. *Current Biology*, *24*, 1909–1917. https://doi.org/10.1016/j.cub.2014.07.001

Chan, D., McIntyre, A. D., Hegele, R. A., & Don-Wauchope, A. C. (2016). Familial partial lipodystrophy presenting as metabolic syndrome. *Journal of Clinical Lipidology*, *10*, 1488–1491. https://doi.org/10.1016/j.jacl.2016.08.012

Chao, B., Li, B. X., & Xiao, X. (2017). Design, synthesis and evaluation of antitumor acylated monoaminopyrroloquinazolines. *Bioorganic & Medicinal Chemistry Letters*, *27*, 3107–3110. https://doi.org/10.1016/j.bmcl.2017.05.038

Chockalingam, P., Clur, S. A., Breur, J. M., Kriebel, T., Paul, T., Rammeloo, L. A., Wilde, A. A., & Blom, N. A. (2012). The diagnostic and therapeutic aspects of loss-of-function cardiac sodium channelopathies in children. *Heart Rhythm: the Official Journal of the Heart Rhythm Society*, *9*, 1986–1992. https://doi.org/10.1016/j.hrthm.2012.08.011

Dhe-Paganon, S., Werner, E. D., Chi, Y. I., & Shoelson, S. E. (2002). Structure of the globular tail of nuclear lamin. *Journal of Biological Chemistry*, *277*, 17381–17384. https://doi.org/10.1074/jbc.C200038200

Haas, M., & Jost, E. (1993). Functional analysis of phosphorylation sites in human lamin A controlling lamin disassembly, nuclear transport and assembly. *European Journal of Cell Biology*, *62*, 237–247.

Heitlinger, E., Peter, M., Lustig, A., Villiger, W., Nigg, E. A., & Aebi, U. (1992). The role of the head and tail domain in lamin structure and assembly: Analysis of bacterially expressed chicken lamin A and truncated B2 lamins. *Journal of Structural Biology*, *108*, 74–89.

Hermida-Prieto, M., Monserrat, L., Castro-Beiras, A., Laredo, R., Soler, R., Peteiro, J., Rodriguez, E., Bouzas, B., Alvarez, N., Muniz, J., & Crespo-Leiro, M. (2004). Familial dilated cardiomyopathy and isolated left ventricular noncompaction associated with lamin A/C gene mutations. *The American Journal of Cardiology*, *94*, 50–54. https://doi.org/10.1016/j.amjcard.2004.03.029

Ho, C. Y., & Lammerding, J. (2012). Lamins at a glance. *Journal of Cell Science*, *125*, 2087–2093. https://doi.org/10.1242/jcs.087288

Holst, A. G., Liang, B., Jespersen, T., Bundgaard, H., Haunso, S., Svendsen, J. H., & Tfelt-Hansen, J. (2010). Sick sinus syndrome, progressive cardiac conduction disease, atrial flutter and ventricular tachycardia caused by a novel SCN5A mutation. *Cardiology*, *115*, 311–316. https://doi.org/10.1159/000312747

Houben, F., De Vos, W. H., Krapels, I. P., Coorens, M., Kierkels, G. J., Kamps, M. A., Verstraeten, V. L., Marcelis, C. L., van

den Wijngaard, A., Ramaekers, F. C., & Broers, J. L. (2013). Cytoplasmic localization of PML particles in laminopathies. *Histochemistry and Cell Biology*, *139*, 119–134. https://doi.org/10.1007/s00418-012-1005-5

Keller, H., Finsterer, J., Steger, C., Wexberg, P., Gatterer, E., Khazen, C., Stix, G., Gerull, B., Hoftberger, R., & Weidinger, F. (2012). Novel c.367_369del LMNA mutation manifesting as severe arrhythmias, dilated cardiomyopathy, and myopathy. *Heart and Lung*, *41*, 382–386. https://doi.org/10.1016/j.hrtlng.2011.07.007

Kochin, V., Shimi, T., Torvaldson, E., Adam, S. A., Goldman, A., Pack, C. G., Melo-Cardenas, J., Imanishi, S. Y., Goldman, R. D., & Eriksson, J. E. (2014). Interphase phosphorylation of lamin A. *Journal of Cell Science*, *127*, 2683–2696. https://doi.org/10.1242/jcs.141820

Krimm, I., Ostlund, C., Gilquin, B., Couprie, J., Hossenlopp, P., Mornon, J. P., Bonne, G., Courvalin, J. C., Worman, H. J., & Zinn-Justin, S. (2002). The Ig-like structure of the C-terminal domain of lamin A/C, mutated in muscular dystrophies, cardiomyopathy, and partial lipodystrophy. *Structure*, *10*, 811–823. https://doi.org/10.1016/S0969-2126(02)00777-3

Kumar, S., Baldinger, S. H., Gandjbakhch, E., Maury, P., Sellal, J. M., Androulakis, A. F., Waintraub, X., Charron, P., Rollin, A., Richard, P., Stevenson, W. G., Macintyre, C. J., Ho, C. Y., Thompson, T., Vohra, J. K., Kalman, J. M., Zeppenfeld, K., Sacher, F., Tedrow, U. B., & Lakdawala, N. K. (2016). Long-term arrhythmic and nonarrhythmic outcomes of Lamin A/C mutation carriers. *Journal of the American College of Cardiology*, *68*, 2299–2307. https://doi.org/10.1016/j.jacc.2016.08.058

Lee, Y. S., Olaopa, M. A., Jung, B. C., Lee, S. H., Shin, D. G., Park, H. S., Cho, Y., Han, S. M., Lee, M. H., & Kim, Y. N. (2016). Genetic variation of SCN5A in Korean patients with sick sinus syndrome. *Korean Circulation Journal*, *46*, 63–71. https://doi.org/10.4070/kcj.2016.46.1.63

Li, B. X., Chen, J., Chao, B., David, L. L., & Xiao, X. (2018). Anticancer pyrroloquinazoline LBL1 targets nuclear lamins. *ACS Chemical Biology*. https://doi.org/10.1021/acschembio.8b00266

Liu, Z., Shan, H., Huang, J., Li, N., Hou, C., & Pu, J. (2016). A novel lamin A/C gene missense mutation (445 V > E) in immunoglobulin-like fold associated with left ventricular noncompaction. *Europace*, *18*, 617–622. https://doi.org/10.1093/europace/euv044

Makita, N. (2009). Phenotypic overlap of cardiac sodium channelopathies: Individual-specific or mutation-specific? *Circulation Journal*, *73*, 810–817.

Malek, L. A., Labib, S., Mazurkiewicz, L., Saj, M., Ploski, R., Tesson, F., & Bilinska, Z. T. (2011). A new c.1621 C > G, p. R541G lamin A/C mutation in a family with DCM and regional wall motion abnormalities (akinesis/dyskinesis): Genotype-phenotype correlation. *Journal of Human Genetics*, *56*, 83–86. https://doi.org/10.1038/jhg.2010.137

Markandeya, Y. S., Tsubouchi, T., Hacker, T. A., Wolff, M. R., Belardinelli, L., & Balijepalli, R. C. (2016). Inhibition of late sodium current attenuates ionic arrhythmia mechanism in ventricular myocytes expressing LaminA-N195K mutation. *Heart Rhythm: the Official Journal of the Heart Rhythm Society*, *13*, 2228–2236. https://doi.org/10.1016/j.hrthm.2016.08.007

Mitsuhashi, H., Hayashi, Y. K., Matsuda, C., Noguchi, S., Wakatsuki, S., Araki, T., & Nishino, I. (2010). Specific phosphorylation of Ser458 of A-type lamins in LMNA-associated myopathy patients. *Journal of Cell Science*, *123*, 3893–3900. https://doi.org/10.1242/jcs.072157

Mounkes, L. C., Kozlov, S. V., Rottman, J. N., & Stewart, C. L. (2005). Expression of an LMNA-N195K variant of A-type lamins results in cardiac conduction defects and death in mice. *Human Molecular Genetics*, *14*, 2167–2180. https://doi.org/10.1093/hmg/ddi221

Olaopa, M. A., Spoonamore, K. G., Bhakta, D., Chen, Z., Celestino-Soper, P. B. S., Chen, P. S., Ai, T., & Vatta, M. (2018). Lamin A/C variants found in patients with cardiac conduction disease reduce sodium currents. *Cardiogenetics*, *8*, 4–8. https://doi.org/10.4081/cardiogenetics.2018.7127

Osmanagic-Myers, S., Dechat, T., & Foisner, R. (2015). Lamins at the crossroads of mechanosignaling. *Genes & Development*, *29*, 225–237. https://doi.org/10.1101/gad.255968.114

Pethig, K., Genschel, J., Peters, T., Wilhelmi, M., Flemming, P., Lochs, H., Haverich, A., & Schmidt, H. H. (2005). LMNA mutations in cardiac transplant recipients. *Cardiology*, *103*, 57–62. https://doi.org/10.1159/000082048

Saj, M., Jankowska, A., Lewandowski, M., Szwed, H., Szperl, M., Ploski, R., & Bilinska, Z. T. (2010). Dilated cardiomyopathy with profound segmental wall motion abnormalities and ventricular arrhythmia caused by the R541C mutation in the LMNA gene. *International Journal of Cardiology*, *144*, e51–53. https://doi.org/10.1016/j.ijcard.2008.12.083

Samani, K., Ai, T., Towbin, J. A., Brugada, R., Shuraih, M., Xi, Y., Wu, G., Cheng, J., & Vatta, M. (2009). A nonsense SCN5A mutation associated with Brugada-type electrocardiogram and intraventricular conduction defects. *Pacing and Clinical Electrophysiology*, *32*, 1231–1236. https://doi.org/10.1111/j.1540-8159.2009.02470.x

Samani, K., Wu, G., Ai, T., Shuraih, M., Mathuria, N. S., Li, Z., Sohma, Y., Purevjav, E., Xi, Y., Towbin, J. A., Cheng, J., & Vatta, M. (2009). A novel SCN5A mutation V1340I in Brugada syndrome augmenting arrhythmias during febrile illness. *Heart Rhythm: the Official Journal of the Heart Rhythm Society*, *6*, 1318–1326. https://doi.org/10.1016/j.hrthm.2009.05.016

Sasse, B., Aebi, U., & Stuurman, N. (1998). A tailless Drosophila lamin Dm0 fragment reveals lateral associations of dimers. *Journal of Structural Biology*, *123*, 56–66. https://doi.org/10.1006/jsbi.1998.4006

Shaw, T., Elliott, P., & McKenna, W. J. (2002). Dilated cardiomyopathy: A genetically heterogeneous disease. *Lancet*, *360*, 654–655. https://doi.org/10.1016/S0140-6736(02)09879-3

Shumaker, D. K., Solimando, L., Sengupta, K., Shimi, T., Adam, S. A., Grunwald, A., Strelkov, S. V., Aebi, U., Cardoso, M. C., & Goldman, R. D. (2008). The highly conserved nuclear lamin Ig-fold binds to PCNA: Its role in DNA replication. *Journal of Cell Biology*, *181*, 269–280. https://doi.org/10.1083/jcb.200708155

Shuraih, M., Ai, T., Vatta, M., Sohma, Y., Merkle, E. M., Taylor, E., Li, Z., Xi, Y., Razavi, M., Towbin, J. A., & Cheng, J. (2007). A common SCN5A variant alters the responsiveness of human sodium channels to class I antiarrhythmic agents. *Journal of Cardiovascular Electrophysiology*, *18*, 434–440. https://doi.org/10.1111/j.1540-8167.2007.00777.x

Stroud, M. J., Banerjee, I., Veevers, J., & Chen, J. (2014). Linker of nucleoskeleton and cytoskeleton complex proteins in cardiac structure, function, and disease. *Circulation Research*, *114*, 538–548. https://doi.org/10.1161/CIRCRESAHA.114.301236

Stuurman, N., Heins, S., & Aebi, U. (1998). Nuclear lamins: Their structure, assembly, and interactions. *Journal of Structural Biology*, *122*, 42–66. https://doi.org/10.1006/jsbi.1998.3987

Swift, J., & Discher, D. E. (2014). The nuclear lamina is mechano-responsive to ECM elasticity in mature tissue. *Journal of Cell Science*, *127*, 3005–3015. https://doi.org/10.1242/jcs.149203

Torvaldson, E., Kochin, V., & Eriksson, J. E. (2015). Phosphorylation of lamins determine their structural properties and signaling functions. *Nucleus*, *6*, 166–171. https://doi.org/10.1080/19491034.2015.1017167

Wang, D. W., Viswanathan, P. C., Balser, J. R., George Jr., A. L., & Benson, D. W. (2002). Clinical, genetic, and biophysical characterization of SCN5A mutations associated with atrioventricular conduction block. *Circulation*, *105*, 341–346.

Wu, W., Muchir, A., Shan, J., Bonne, G., & Worman, H. J. (2011). Mitogen-activated protein kinase inhibitors improve heart function and prevent fibrosis in cardiomyopathy caused by mutation in lamin A/C gene. *Circulation*, *123*, 53–61. https://doi.org/10.1161/CIRCULATIONAHA.110.970673

Yu, C. C., Ai, T., Weiss, J. N., & Chen, P. S. (2014). Apamin does not inhibit human cardiac Na^+ current, L-type Ca^{2+} current or other major K^+ currents. *PLoS One*, *9*, e96691. https://doi.org/10.1371/journal.pone.0096691

Zaragoza, M. V., Fung, L., Jensen, E., Oh, F., Cung, K., McCarthy, L. A., Tran, C. K., Hoang, V., Hakim, S. A., & Grosberg, A. (2016). Exome sequencing identifies a novel LMNA splice-site mutation and multigenic heterozygosity of potential modifiers in a family with sick sinus syndrome, dilated cardiomyopathy, and sudden cardiac death. *PLoS One*, *11*, e0155421. https://doi.org/10.1371/journal.pone.0155421

Ziane, R., Huang, H., Moghadaszadeh, B., Beggs, A. H., Levesque, G., & Chahine, M. (2010). Cell membrane expression of cardiac sodium channel Na(v)1.5 is modulated by alpha-actinin-2 interaction. *Biochemistry*, *49*, 166–178. https://doi.org/10.1021/bi901086v